

# Magnetic field-induced entropy change in phase-separated manganites

G. J. Liu, J. R. Sun,<sup>a)</sup> J. Z. Wang, and B. G. Shen

State Key Laboratory for Magnetism, Institute of Physics, Chinese Academy of Sciences, Beijing 100080, People's Republic of China

(Received 5 June 2006; accepted 18 October 2006; published online 29 November 2006)

Magnetic field-induced entropy change has been experimentally studied for phase-separated manganites  $\text{Eu}_{0.55}\text{Sr}_{0.45}\text{MnO}_3$  and  $\text{La}_{0.27}\text{Nd}_{0.40}\text{Ca}_{0.33}\text{MnO}_3$ . The entropy derived from the measured heat capacity exhibits a significant decrease under applied field in a broad temperature range below Curie temperature, and the maximum change is  $\sim 8$  J/kg K for  $\text{Eu}_{0.55}\text{Sr}_{0.45}\text{MnO}_3$  and is  $\sim 4.2$  J/kg K for  $\text{La}_{0.27}\text{Nd}_{0.40}\text{Ca}_{0.33}\text{MnO}_3$  for a field change of 0–5 T. In comparison with the calorimetric technique, Maxwell relation fails to give a proper description for the entropy change. It underestimates the entropy reduction in the low temperature range and even anticipates an entropy increase for  $\text{Eu}_{0.55}\text{Sr}_{0.45}\text{MnO}_3$ . Failures of the Maxwell relation could be ascribed to the coexistence of two phases in the compound and to the variation of the proportion of each phase with applied field. © 2006 American Institute of Physics. [DOI: 10.1063/1.2397535]

Room-temperature magnetic refrigeration has been pursued for decades due to its environment friendly nature and high efficiency. Discovery of giant magnetocaloric effect (GMCE) in  $\text{Gd}_5\text{Si}_{4-x}\text{Ge}_x$ ,  $\text{LaFe}_{11.2}\text{Co}_{0.7}\text{Si}_{1.1}$ , and  $\text{MnFeP}_x\text{As}_{1-x}$  made the reality closer to goal and stimulated an extensive exploration of potential magnetocaloric materials in recent years.<sup>1–3</sup>

Different from the intensively studied paramagnetic (PM) or ferromagnetic (FM) materials that undergo a second-order magnetic transition, room-temperature GMCE always occurs in materials that exhibit a first-order magnetic transition. In this case magnetic field drives Curie temperature upwards or downwards, giving rise to a giant entropy change concentrated within a narrow temperature range around  $T_C$ .

Magnetic entropy change can be estimated from magnetization data based on the well known Maxwell relation or from heat capacity under various magnetic fields. Due to its simplicity and convenience, the former has been widely used though there are arguments about its applicability to first-order phase transition.<sup>4</sup> It is fortunate that the Maxwell relation has been proven to give the same results as heat capacity for most of the compounds studied.<sup>5</sup> Therefore, this approach has usually been used without verification even when the system experiences complex phase transitions.<sup>6</sup> In fact, if two or more phases coexist in the compound, the applicability of the Maxwell relation should be checked carefully considering the fact that this relation is derived for a homogeneous system in an equilibrium state. In this letter, we showed that the entropy change estimated by the Maxwell relation is substantially different from that deduced from heat capacity for phase-separated manganites, and the actual entropy change well below the Curie temperature can be either overestimated or underestimated.

Two polycrystalline samples  $\text{Eu}_{0.55}\text{Sr}_{0.45}\text{MnO}_3$  (ESMO) and  $\text{La}_{0.27}\text{Nd}_{0.40}\text{Ca}_{0.33}\text{MnO}_3$  (LNCMO) were prepared by the conventional solid state reaction method. Well mixed stoichiometric  $\text{Eu}_2\text{O}_3$ ,  $\text{La}_2\text{O}_3$ ,  $\text{Nd}_2\text{O}_3$ ,  $\text{SrCO}_3$ ,  $\text{CaCO}_3$ , and

$\text{MnO}_2$  were calcinated at 900 °C for 10 h. The resultant products were ground, pelletized, and sintered at 1350 °C for 48 h with an intermediate regrinding for homogenization. The samples thus obtained are single phase as confirmed by the Rietveld refinement of the x-ray diffraction spectra.

Magnetization of the sample was determined as a function of temperature by a superconducting quantum interference device magnetometer. The sample was cooled to a pre-setting temperature, then a magnetic field was applied and magnetization was measured in the following warming process. This procedure was repeated under an incremented magnetic field after each thermal cycle to avoid the effects of magnetic history. Figure 1 shows the temperature-dependent magnetization of ESMO measured under the fields between 0.1 and 5 T (top panel). Two magnetic processes take place

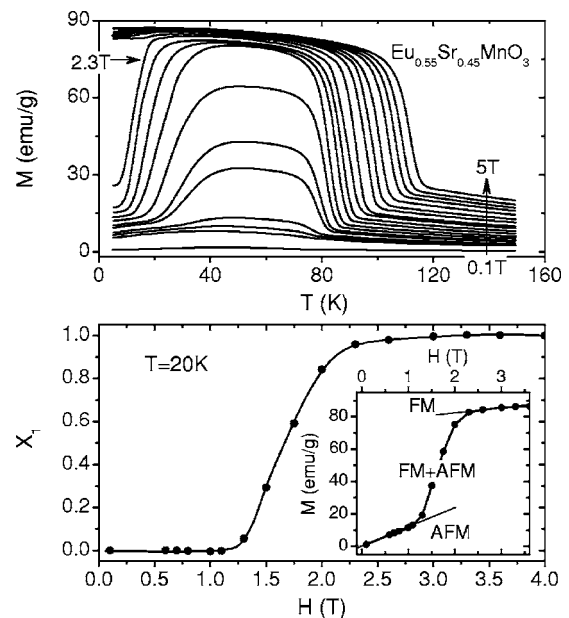


FIG. 1. Thermal magnetization of  $\text{Eu}_{0.55}\text{Sr}_{0.45}\text{MnO}_3$  measured under different magnetic fields (top panel) and the proportion of the FM phase ( $X_1$ ) as a function of magnetic field at a selected temperature of 20 K (bottom panel). Bottom inset shows the corresponding isothermal magnetization curve for  $T=20$  K. The solid lines are guides for the eyes.

<sup>a)</sup> Author to whom correspondence should be addressed; electronic mail: jrsun@g203.iphy.ac.cn

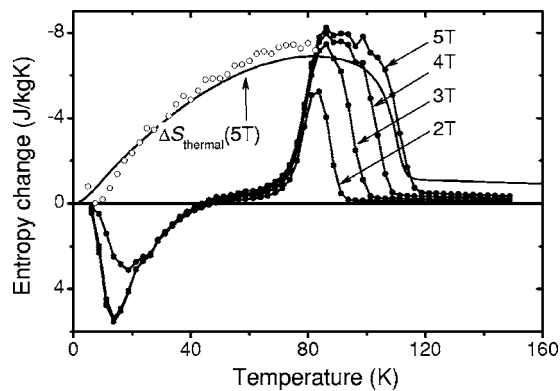


FIG. 2. Entropy changes in  $\text{Eu}_{0.55}\text{Sr}_{0.45}\text{MnO}_3$  determined by Maxwell relation (solid symbols), specific heat (solid lines), and the extra two terms plus the Maxwell result (open circles), respectively.

sequentially with the decrease of temperature. The first one is a PM to FM transition at a high temperature, and the second one is a FM to antiferromagnetic (AFM) transition at a low temperature. In the intermediate temperature and magnetic field range FM and AFM phases coexist, which is similar to the compounds  $\text{La}_{0.19}\text{Bi}_{0.35}\text{Ca}_{0.33}\text{MnO}_3$  (Ref. 7) and  $\text{Nd}_{0.5}\text{Ca}_{0.5}\text{MnO}_3$ ,<sup>8</sup> while the PM and FM phases coexist between  $\sim 80$  and  $\sim 120$  K under the fields from 0 to 5 T. It is obvious that the proportion of each phase, which can be calculated based on the magnetization isotherms, should be a function of external field. The bottom panel of Fig. 1 displays the variation of the FM population with magnetic field at a fixed temperature of 20 K. The compound is AFM below 1 T, and transits to the FM state when the applied field exceeds  $\sim 1.2$  T. The fully FM polarized state is obtained above  $\sim 2.25$  T. Similar behaviors are observed at other temperatures below 80 K.

Figure 2 shows the entropy change calculated by the Maxwell relation [ $\Delta S_M(T)$ ]. A remarkable feature is the exact correspondence of entropy change to magnetic transition. Magnetic field causes a decrease of magnetic entropy at the first transition and an increase at the second transition. This is apparently a consequence of the field-induced upward and downward shifts of the two transitions, respectively. It is interesting that  $\Delta S_M$  is quite small between  $\sim 40$  and  $\sim 70$  K in spite of the AFM-FM transition in this region (Fig. 1).

The heat capacity of ESMO was measured by a physical property measurement system (PPMS-14H) under two fields of  $H=0$  and 5 T. The experiments were performed in the temperature range from 2 to 200 K with the temperature step of 2 or 3 K near or far away from the magnetic transition. As shown in Fig. 3, heat capacity exhibits a similar feature to that of other manganites.<sup>9</sup> It increases first rapidly and then slowly with the increase of temperature. The  $C_p(T)$  curve for  $H=0$  is rather smooth, without any signature of phase transition. In contrast, a significant peak appears at  $\sim 110$  K under 5 T, corresponding to the field-induced FM transition. Entropy change can be calculated based on the formula  $\Delta S_{\text{heat}} = \int_0^T [C_p(T, H) - C_p(T, 0)] dT/T$ , and the results thus obtained are also shown in Fig. 2. It is small at low temperatures and grows monotonically with the increase of temperature until a broad maximum of  $\sim 7$  J/kg K at  $\sim 85$  K. Further increase in temperature leads to a rapid decrease of  $\Delta S_{\text{heat}}$ . It is surprising that there is a significant discrepancy between the entropies calculated, respectively, from the calorimetric and the magnetization data in the low temperature

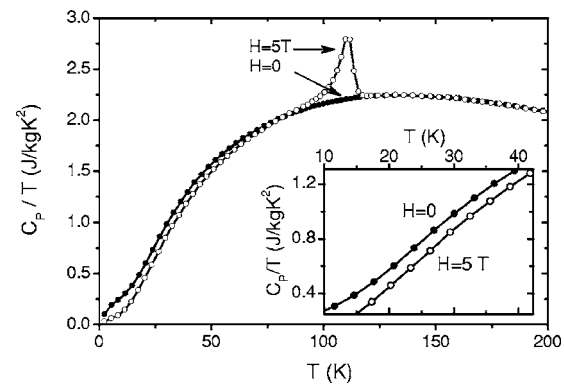


FIG. 3. Heat capacity of  $\text{Eu}_{0.55}\text{Sr}_{0.45}\text{MnO}_3$  measured under the fields of  $H=0$  and 5 T. The inset plot is a close view of the heat capacity in the low temperature range.

range though the main features of  $\Delta S_{\text{heat}}$  and  $\Delta S_M$  are almost the same above  $\sim 80$  K. Different from the entropy increase below  $\sim 40$  K suggested by  $|\Delta S_M|$ ,  $\Delta S_{\text{heat}}$  declares an entropy decrease in the whole temperature range below  $\sim 110$  K.

To get the knowledge about the detailed  $C_p$ - $H$  relation, we measured the specific heat of ESMO as a function of magnetic field at two selected temperatures  $\sim 20$  K, where positive  $\Delta S_M$  appears, and 50 K, where  $\Delta S_M \approx 0$ . Similar behaviors are observed at both temperatures. As shown in Fig. 4 (only the results for  $T=20$  K are presented), the heat capacity exhibits a rapid decrease with magnetic field before the saturation for  $H > 3$  T. The maximum change of  $C_p$  is  $\sim 18\%$  at 20 K and is  $\sim 5\%$  at 50 K, well beyond the experiment errors ( $< 1\%$ ). The exact correspondence between  $C_p$  and  $M$  suggests that this is an intrinsic property of ESMO. This result confirms the entropy reduction at low temperatures.

Discrepancy between  $\Delta S_M$  and  $\Delta S_{\text{heat}}$  is also observed in sample LNCMO. Different from ESMO, there is only one field-induced FM transition in LNCMO, which leads to a towerlike entropy change.  $\Delta S_{\text{heat}}$  spans in a much wider temperature range than  $\Delta S_M$ , i.e.,  $\Delta S_M$  underestimates substantially the entropy change below  $\sim 80$  K (Fig. 5).

Differences between  $\Delta S_M$  and  $\Delta S_{\text{heat}}$  can be understood based on a simple analysis on the magnetic and calorimetric data. According to Fig. 1, there would be no detectable phase transition in the case of  $H=0$ , and only one FM transition at  $\sim 114$  K under the field of 5 T for ESMO. These actually imply the absence of entropy anomaly at  $\sim 20$ – $30$  K, where the AFM-FM transition takes place under proper applied fields. In contrast, to get the entropy change by Maxwell

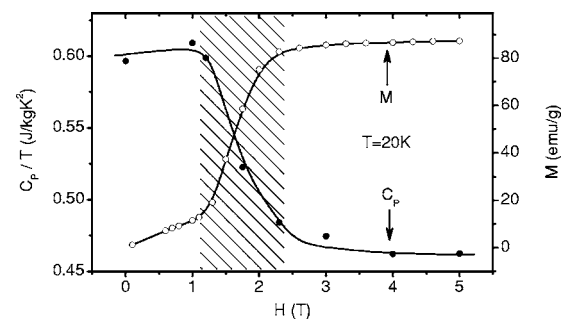


FIG. 4. Heat capacity and isothermal magnetization as functions of magnetic field measured at a fixed temperature of  $T=20$  K. The hatched area marks the AFM-FM transition. The solid lines are guides for the eyes.

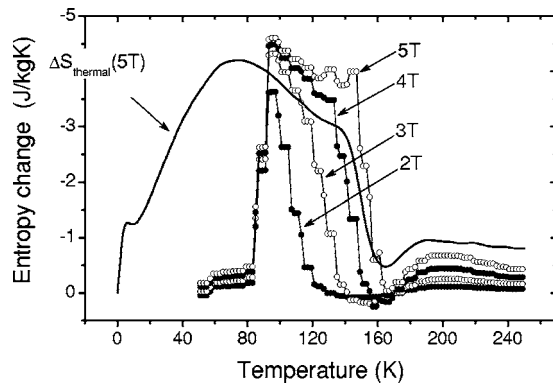


FIG. 5. Entropy changes in  $\text{La}_{0.27}\text{Nd}_{0.40}\text{Ca}_{0.33}\text{MnO}_3$  determined by Maxwell relation (solid symbols) and heat capacity (solid lines), respectively.

relation thermomagnetization curves under different fields have to be used, and the low temperature shift of the AFM-FM transition with applied field causes the positive  $\Delta S_M$  peak around  $\sim 15$  K.

From the magnetic data we know that two phases coexist in ESMO and LNCMO in a wide temperature range under appropriate magnetic field. In this case whether the Maxwell relation can properly describe the relation between entropy and magnetization is suspicious. Based on thermodynamics theory, the entropy change will be

$$\Delta S_{\text{heat}} = X_0 \Delta S_2 + \int_0^T (\Delta X_1 C_{p1} - \Delta X_1 C_{p2}) dT/T, \quad (1)$$

where  $X_0$  is the total volume,  $X_1$  the volume occupied by FM phase, and  $C_{p1}$  and  $C_{p2}$  are the heat capacities (per volume) of the FM and AFM phases, respectively.  $\Delta S_2 = S_2(T, H) - S_2(T, 0)$  and  $\Delta X_1 C_p = X_1(T, H) C_p(T, H) - X_1(T, 0) C_p(T, 0)$  ( $S_2$  the entropy of the AFM phase). In contrast, the Maxwell relation gives

$$\begin{aligned} \Delta S_M = & X_0 \Delta S_2 + \int_0^T (\Delta X_1 C_{p1} - \Delta X_1 C_{p2}) dT/T + \int_0^H (M_1 \\ & - M_2) (\partial X_1 / \partial T)_H dH - \int_0^T dT/T \int_0^H (C_{p1} - C_{p2}) \\ & \times (\partial X_1 / \partial H)_T dH, \end{aligned} \quad (2)$$

where the relation  $M = X_0 M_2 + X_1 (M_1 - M_2)$  has been used. It is obvious that  $\Delta S_{\text{heat}} = \Delta S_M$  is true only when  $X_1$  is independent of  $T$  and  $H$ . In most of the phase-separated compounds,

the field-induced AFM-FM transition does not occur until a threshold field. Below this field, the Maxwell relation can still be used based on the above arguments. However, when the applied field is so large as to affect the proportion of the FM or AFM phase in the compound, calorimetric data have to be used. As shown in Fig. 2 (open circles), the entropy change calculated from the Maxwell relation plus the ‘‘extra’’ two terms does follow the line derived from the calorimetric measurement within the experimental errors.

If the compound stays in an equilibrium state, the two extra terms in Eq. (2) will cancel one another because of the equality of the Gibbs free energies of the coexisted phases. Incomplete cancellation below 80 K implies that the compound may stay in a stable state, rather than in an equilibrium state.

Besides ESMO and LNCMO, there are also many other compounds showing the characters of phase separation. The present work indicates that calorimetric data should be used to estimate the entropy change in phase-separated compound, and significant errors could be introduced by the Maxwell relation when the proportions of coexisted phases can be modified by an external field.

This work has been supported by the National Natural Science Foundation of China, the State Key Project for the Fundamental Research of China.

<sup>1</sup>V. K. Pecharsky and K. A. Gschneidner, Jr., Phys. Rev. Lett. **78**, 4494 (1997).

<sup>2</sup>F. X. Hu, B. G. Shen, J. R. Sun, G. J. Wang, and Z. H. Cheng, Appl. Phys. Lett. **80**, 826 (2002).

<sup>3</sup>O. Tegus, E. Brück, K. H. Buschow, and F. R. de Boer, Nature (London) **415**, 150 (2002).

<sup>4</sup>A. Giguère, M. Foldeaki, B. Ravi Gopal, R. Chahine, T. K. Bose, A. Frydman, and J. Barclay, Phys. Rev. Lett. **83**, 2262 (1999); J. R. Sun, F. X. Hu, and B. G. Shen, *ibid.* **85**, 4191 (2000).

<sup>5</sup>M. Foldeaki, W. Schnelle, E. Gmelin, P. Benard, B. Kozzegi, A. Giguère, R. Chahine, and T. K. Bose, J. Appl. Phys. **82**, 309 (1997); V. K. Pecharsky and K. A. Gschneidner, Jr., *ibid.* **86**, 565 (1999).

<sup>6</sup>P. Chen, Y. W. Du, and G. Ni, Europhys. Lett. **52**, 589 (2000); F. X. Hu, X. L. Qian, G. J. Wang, J. Wang, J. R. Sun, X. X. Zhang, Z. H. Cheng, and B. G. Shen, J. Phys.: Condens. Matter **15**, 3299 (2003); Y. Lu, N. L. Di, G. J. Wang, Q. A. Li, and Z. H. Cheng, *ibid.* **16**, L243 (2004).

<sup>7</sup>J. R. Sun, J. Gao, Y. Fei, R. W. Li, and B. G. Shen, Phys. Rev. B **67**, 144414 (2003).

<sup>8</sup>T. Kimura, R. Kumai, Y. Okimoto, Y. Tomioka, and Y. Tokura, Phys. Rev. B **62**, 15021 (2000).

<sup>9</sup>V. Hardy, A. Maignan, S. Hébert, and C. Martin, Phys. Rev. B **67**, 024401 (2003).